Enhancing Low-Light Sports Motion Images with Improved Bilateral Filtering and Auto MSRCR

Yuxin Lin

Email: Yuxin Liu78@126.com

Physical education teaching and training, Chengdu sport university, Chengdu, 610041, China

Keywords: Sport image processing, physical education, motion blur, bilateral filtering, Gaussian kernel

Received: October 22, 2025

Low-light sports images are very common in night sports games recording, but many details of these images are difficult to analyze. Therefore, this paper proposes a sports image enhancement method based on improved bilateral filtering to solve the problem of image blur of night sports games recording and promote the efficiency of physical education. Firstly, in the HSV color space of the original image, the MSR algorithm is applied to the V component using bilateral filtering for brightness enhancement, preserving the original color information while improving image brightness. Next, the CLAHE algorithm is employed in the LAB color space to enhance details in the initially enhanced brightness image, resulting in a more detailed image. In order to create the enhanced low-light image, the detail-enhanced image is combined with the original low-light image using the Auto MSRCR algorithm and then weighted fusion is carried out. In the end, Wiener filtering is used to process the motion blur information and produce the final processed image. The modified images are compared with the MSR, MSRCR, CLAHE, and improved GAMMA algorithms using evaluation measures such UCIQE, AG, SD, and IE to assess the algorithm's performance. The method achieves significant improvements in both visual quality and objective metrics, such as UCIQE, compared to state-of-the-art methods like MSRCR and CLAHE. Specifically, our method improves the UCIQE score by 65.24%, demonstrating superior preservation of edge details and color balance. We also show that our approach outperforms MSRCR by 35% in reducing halo artifacts and over-enhancement. These results are validated on the LOL dataset, which includes various motion-blur scenarios in sports images.

Povzetek: Predstavljena je metoda za izboljšanje športnih slik v slabi svetlobi z zameglitvijo gibanja z uporabo izboljšanega bilateralnega filtriranja in Auto MSRCR algoritma ter Wienerjevega filtriranja. Metoda učinkovito ohranja barvo in izboljša robne podrobnosti, kar vodi do boljšega indeksa UCIQE v primerjavi z MSRCR, kar potrjuje izjemno vizualno kakovost.

1 Introduction

In the field of sports training, the application of blur detail analysis methods to analyse motion video images holds significant importance as it aims to improve the recognition of motion detail features. Therefore, exploring detail enhancement algorithms for blurry motion video images has a profound impact on the development of the field [12,13]. However, during the process of capturing motion images, images captured in low-light environments are inevitably affected, and the limitations of environmental brightness restrict the acquisition and subsequent application of image information. Therefore, it's imperative to improve low-light photos. The primary goal of image enhancement is to draw attention to pertinent feature information in the image in accordance with the specifications, so enhancing the completeness of the information that has been saved [14].

Traditional image enhancement methods mainly include Retinex and SIFT algorithms based on human visual perception models [15]. Building upon these, researchers have proposed the multi-scale weighted average retina algorithm, which has color restoration capabilities and is applied to enhance blurry details in

motion video images. The Retinex method was developed by Land et al. and is based on the visual system. It enhances an image by breaking it down into reflection and lighting components. The Retinex theory introduced SSR [2] and MSR [3] algorithms, but they suffer from color distortion. To address this issue, researchers subsequently proposed the MSRCR [4] and Auto MSRCR [6] algorithms. Although the MSRCR algorithm eliminates color distortion, it may cause halo artifacts in the image.

In recent years, various methods have been proposed for enhancing images under low-light and motion-blur conditions. These methods, including MSRCR, CLAHE, and Wiener filtering, aim to improve image quality by addressing noise, contrast, and detail preservation. However, these techniques often struggle with overenhancement, halo artifacts, and insufficient edge preservation in motion-blur images.

To address the aforementioned issues, this study proposes a method for enhancing low-brightness images by combining MSR with bilateral filtering and the Auto MSRCR algorithm. To begin with, the initial image is converted from the RGB to the HSV color system, and then Bilateral filtering-based MSR is used to improve the brightness channel, resulting in an enhanced brightness

channel which is merged with the chrominance and saturation channels, forming the initial brightness-enhanced image. Secondly, the initial enhanced image is transformed from HSV space to the LAB color space, and CLAHE [5] is employed to enhance the image details. Lastly, the AutoMSRCR algorithm is applied to the original image, producing an image with color whitening but smooth tonal transitions. This image is then weighted fused with the detail-enhanced image, and finally, to get the final improved sports motion image, Wiener filtering is used. Images enhanced using this method demonstrate good results in terms of color, clarity, edge details, and texture, which are more consistent with subjective human perception.

2 Algorithmic theory

2.1 Retinex

The Retinex [1] theory posits that the human visual information system (Human Visual System, HVS) perceives objects primarily due to their reflective properties. The perception of color and brightness is a result of the reflected information generated by objects under different lighting conditions, which is then received by the human eye. Based on this, Land et al. established a mathematical model for this theory, which is represented by the following equation:

$$S(x, y) = R(x, y) \cdot L(x, y) \tag{1}$$

Since an image is composed of pixels, the equation uses x and y to represent the coordinates in the twodimensional image space. The theory assumes that the image of the object's reflected light entering the human eye is represented by S(x, y), while the incident image created by lighting from different angles is represented by L(x, y). The reflectance formed by the object's reflection is denoted as R(x, y), and it is determined solely by the object itself, unaffected by the incident light. The singlescale Retinex (SSR) mentioned above convolves original image with a Gaussian filter to simulate the ambient illumination component. However, single-scale methods may introduce some biases in the original illumination component. Therefore, the multi-scale Retinex algorithm (MSR) employs multiple convolution kernels to convolve with the original image and assigns weights to each scale.

2.2 Auto MSRCR

After applying the MSR algorithm for image enhancement, there can be color distortion in the resulting image. To address the issue of color distortion in the MSR algorithm, a corresponding color restoration function is introduced, forming a new enhancement algorithm known as the MSRCR algorithm [4]. This is how the formula is shown:

$$R_{MSRCR\ i(x,y)} = C_i(x,y)R_{MSR\ i(x,y)}(2)$$

Where: C_i is the color recovery factor. Final MSRCR algorithm:

$$R_{MSRCR i(x,y)} = G[C_i(x,y)R_{MSRCR i(x,y)} + b](3)$$

To achieve adaptive adjustment of image colors, the Auto MSRCR algorithm [6] was proposed. This algorithm's primary goal is to eliminate the RGB values' maximum and minimum parts by 5% using the MSRCR approach. Subsequently, the remaining values are rescaled to the range of [0, 255], resulting in an enhanced image after Auto MSRCR processing. This method eliminates the dependence of the original algorithm on the tonal range of the original image. Auto MSRCR primarily combines MSR to improve the issue of color distortion in images. Algorithm flow is illustrated in Figure 1.

The principle of automatic levels adjustment is shown: Firstly, histogram of the image is calculated to determine the region where the Gray levels are concentrated. Based on this information, the upper threshold value (Tmax) and the lower threshold value (Tmin) for automatic levels adjustment are computed. During the processing, if a pixel value exceeds Tmax, the exceeding portion is set to 255. Conversely, if a pixel value is below Tmin, the lower portion is set to 0. This is how the formula is shown:

$$T_{min} = max(n), n < 0$$

$$count(n) < count(n_0) * \beta$$

$$T_{max} = max(n), n < 0$$

$$count(n) < count(n_0) * \beta$$

Where n represents the value after logarithmic operation, n_0 is set to 0, count indicates the position of U after histogram calculation, and β is a controllable parameter for levels adjustment. In this paper, β is set to 0.05. The final image is stored in the logarithmic domain following processing by the AutoMSRCR algorithm. Using linear normalization, the following formula yields the final improved image in the real number domain. The following is the quantization formula:

$$R(x,y) = (\overline{R}(x,y) - min)/(max - min) * 255(6)$$

Where R(x,y) is the image after the color gain, max represents the maximum value selected for each channel, and min represents the minimum value selected for each channel.

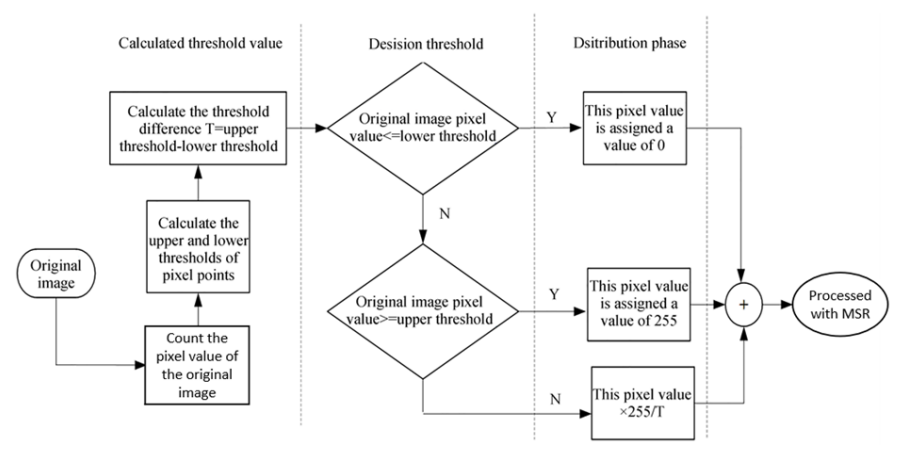


Figure 1. Auto MSRCR flow chart of the algorithm processing

3 **Method**

Algorithm 1: MSR low-illumination enhancement algorithm based on improved bilateral filtering.

Algorithm 1 MSR low-illumination enhancement algorithm based on improved bilateral filtering

Input: Image I

Output: Enhanced Image I'

- 1: Image I as H S V;
- 2: Enhance the V channel of the original image I in the HSV color space;
- 3: S and H channels fused:
- 4: Enhanced image via the CLAHE for luminance;
- 5: Combined weighted with the luminance-improved image;

This research suggests an enhanced low-light picture enhancement technique based on modified bilateral filtering to overcome the shortcomings of the Retinex algorithm. Three primary phases comprise the algorithm: The first step involves applying the modified bilateral filtering MSR method to enhance the V channel of the original image in the HSV color space. The original S and H channels are fused with the resultant luminance channel to create the luminance-enhanced image that was initially obtained. Second, to improve the details in the L channel

of the LAB color space, the luminance-enhanced image is run via the CLAHE [6] algorithm. The improved image with better luminance and details is then obtained by converting the LAB color system back to the RGB color space. Finally, the original low-light image is subjected to the Auto MSRCR method. To create the final enhanced image, the processed output is combined weighted with the luminance-improved image from the second phase. In Figure 2 and Algorithm 1, the general algorithm flow is shown.

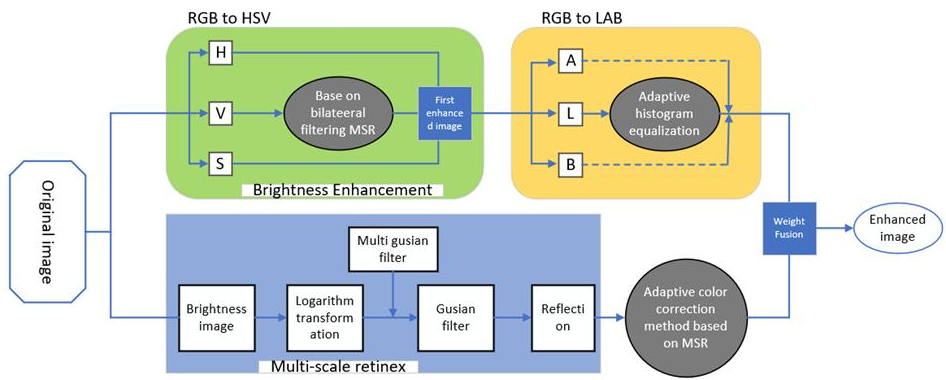


Figure 2: Algorithm flow chart

3.1 **MSR** low-illumination enhancement algorithm based on improved bilateral filtering

One way to convey the information contained in each pixel in the RGB color space as a color space expression is to use the HSV color space. Hue, saturation, and value

are represented in this space, respectively, by the letters H, S, and V [8,16]. The color information of the image remains unaffected when the V channel is adjusted during image enhancement processing. This article uses the HSV color space to divide the image into its three channels, addressing the possible color distortion in the MSR algorithm during processing. The V component is extracted and enhanced for luminance. Subsequently, the enhanced V channel is merged with the original H and S channels, resulting in a luminance-enhanced image that

preserves the original color information. The specific comparison of the effects is illustrated in Figure 3.







(c)HSV Enhanced

Figure 3: Enhanced contrast based on RGB and HSV

Bilateral filtering is then utilized in this work to model the lighting component. As seen in Figure 4, we performed a comparison with Gaussian and median filtering to assess the superiority of the suggested approach.

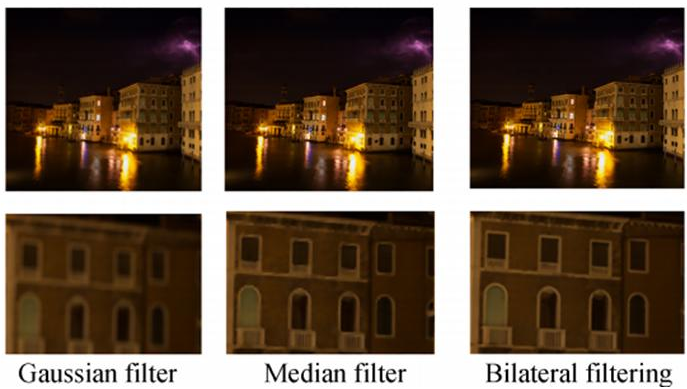


Figure 4: Compare the different filter details

After a comparative analysis, it can be observed that the Gaussian filtering results in an unsatisfactory outcome in terms of detail enlargement, causing the overall image to appear blurry. The median filtering produces a clearer image compared to Gaussian filtering, but there are still missing details in the edge regions of the image. On the other hand, the image processed with bilateral filtering exhibits sharp edge details. Therefore, converting the Gaussian filtering of the MSR algorithm to bilateral filtering for image enhancement better preserves the edge details of the image. The mathematical model of bilateral filtering is represented by the following formula:

$$\bar{I}_{(y)} = \frac{1}{W_p} \sum_{x \in \mathcal{S}} I(x) G_d(x, y) G_r(I(x), I(y))$$
(7)

In this case, S stands for the collection of nearby pixels that are filtered. The target pixel's locations inside the neighborhood are indicated by x and y. I(x) represents the values of each pixel in the set S, whereas I(y) represents the values of the pixels that are retrieved for each pixel position following the filtering operation. G_d and G_r , in bilateral filtering, indicate the geometric space as well as the absolute difference between the gray values of a point in the neighborhood and the center point. W_p shows how these two parameters have been normalized, and the expression is as follows:

$$G_{d} = e^{\frac{\|x-y\|^{2}}{2\sigma_{d}^{2}}}$$

$$G_{r} = e^{\frac{\|I(x)-I(y)\|^{2}}{2\sigma_{r}^{2}}} (8)$$

$$W_{p} = \sum_{x \in s} G_{d} \cdot G_{r}$$

The improved bilateral filtering method used in this study operates by filtering each pixel based on its spatial and intensity similarity. The parameters, including the spatial standard deviation and intensity range , were chosen through empirical tuning. Specifically, σ was set to 2.0 to maintain sharp edges without over-smoothing, while standard deviation was set to 0.1 to preserve color contrast. The Auto MSRCR algorithm was combined with CLAHE for local contrast enhancement. For CLAHE, the clip limit was set to 2.0, and the grid size was 8x8, as these parameters were found to yield the best trade-off between detail preservation and noise reduction in preliminary experiments.

3.2 Image detail processing

In the proposed method, we utilize the CLAHE algorithm, which is primarily based on histogram equalization to reduce noise amplification and enhance local contrast transitions in images. However, it also involves suppressing certain grayscale levels to achieve clearer image processing.

Make numerous sub-regions out of the image, with each image representing a number of sub-regions. The number of pixels in each sub-region is denoted by M.

Calculate grayscale histogram for each sub-region.

Perform histogram clipping on each sub-region, as illustrated in Figure 5. Set a threshold range, and clip the pixels exceeding this range, transferring them to the lower range. Set a threshold value, G, $H_i \ge G$, $H_i = H_{max}$; $H_i <$ $G, H_i = H_{max}.$

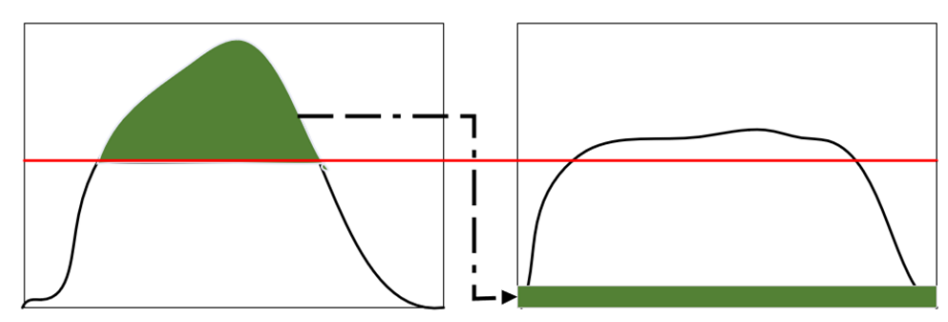


Figure 5: Hearing histogram

Next, we apply regional histogram equalization to each sub-region, where adaptive histogram equalization is performed using interpolation operations [5], as shown in Figure 6. For each block, we calculate its histogram, cumulative distribution function (CDF) [25], and the corresponding transformation function. In the figure, the transformation function at the center of the block (left red square) adheres to the original definition, and the pixel

values in the purple area are obtained through bilinear interpolation using four transformation functions to determine the pixel at the center. The pixel values in the green area are obtained through linear interpolation using the transformation functions of the adjacent two regions, while the pixels in the red area are obtained using their own transformation function.

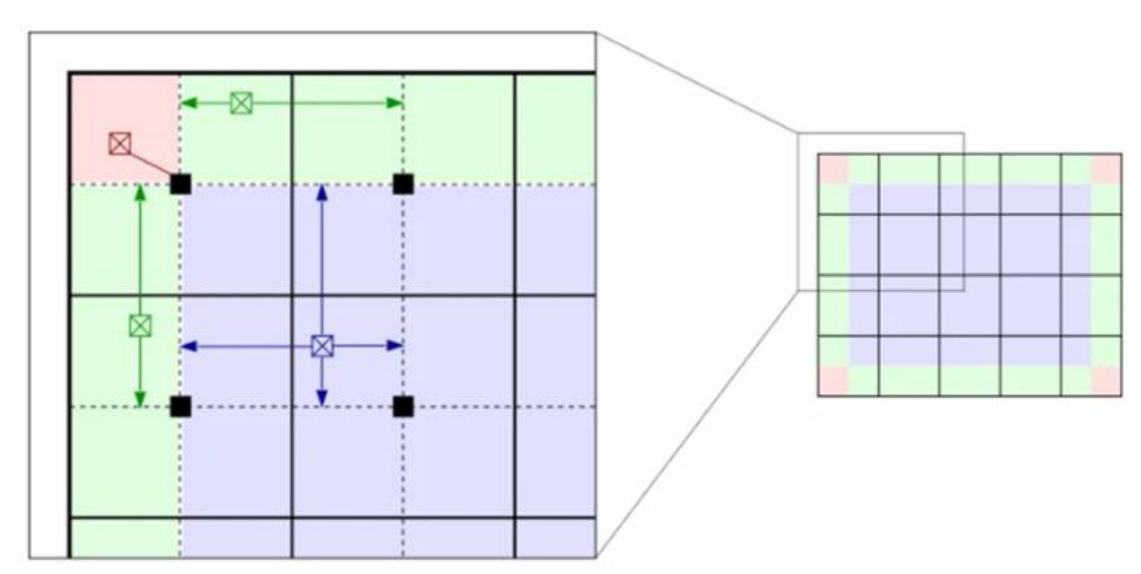


Figure 6: Interpolation operation

In this paper, CLAHE is applied only to the L channel for detail enhancement, preserving the original color information of the enhanced image, as shown in Figure 7. Following the application of the aforementioned two algorithms, weighted fusion with the following formula yields the final enhanced image:

$$R_i(x, y) = mR_{1i}(x, y) + (1 - m)R_{2i}(x, y)(9)$$

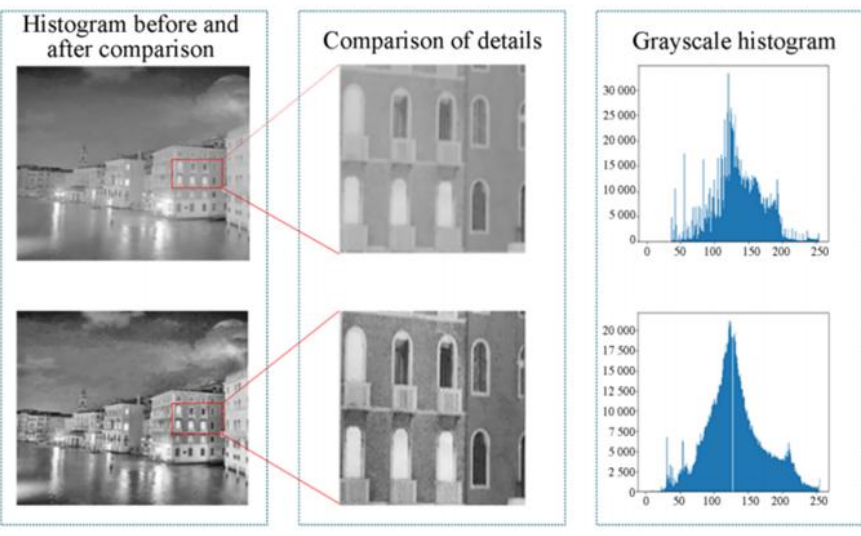


Figure 7: Histogram equalization before and after the comparison

3.3 Motion blur enhancement

Motion blur refers to the phenomenon of image blurring caused by the movement of the camera or objects [17-19]. Assuming that an object or camera moves from position x_0 to position x_1 within a certain period of time, the blur during that time period can be described as:

$$h(t) = \begin{cases} \frac{1}{t_{\text{exposure}}}, & 0 \le t \le t_{\text{exposure}} \\ \mathbf{0}, & \text{otherwise} \end{cases}$$
(10)

Here, the exposure time, or the amount of time the camera lens is left open, is represented by the letter $t_{\rm exposure}$ [26]. This function illustrates that during the exposure time of a moving object or camera, the object's image undergoes a certain displacement within the image plane, resulting in image blur. In spatial domain, this function can be represented as:

$$h(x,y) = \begin{cases} \frac{1}{t_{\text{exposwe}}}, & \text{if } ax + by + c \leq 0\\ 0, & \text{otherwise} \end{cases}$$
 (11)

Here, a, b, c are parameters describing the motion direction and velocity. It can be observed that this function is represented as a linear function in image plane, depicting the motion direction and velocity of the object's image within the image plane during the camera exposure time. Assuming that the motion-blurred image can be obtained through convolution operations, the image calculation can be expressed as follows:

$$g(x,y) = h(x,y) * f(x,y) = \iint_{-\infty}^{\infty} h(\xi,\eta) f(x - \xi, y - \eta) d\xi d\eta$$
(12)

In this case, g(x,y) denotes the motion blur function, f(x,y) represents the original image, and h(x,y) represents the blurred image.

In this article, we construct a Wiener filter to enhance motion blur in images. The core idea is based on a locally weighted regression method. It estimates the value of the target variable by using neighbouring samples that are close in distance to the sample point. Specifically, for a given data point that needs to be predicted, the Wiener filter calculates the distance between that point and each sample point in the training data and assigns weights based on the distance. Sample points that are closer in distance are assigned greater weights, while sample points that are farther away are assigned smaller weights. In this way, the Wiener filter smoothest [20] the estimation of the target variable of the neighbouring samples through weighted averaging, resulting in the predicted value of the data point. The specific steps is shown:

To get the motion blur filter, we first apply the Fourier transform. This is the precise formula:

$$H(u, v) = \mathcal{F}(MotionKernel)(13)$$

Where \mathcal{F} represents the Fourier transform, H(u,v) represents the frequency domain matrix of the motion blur filter, and MotionKernel represents the motion blur kernel generated in the previous step. Afterwards, Gaussian noise is added to the image, and the noise component is obtained by subtracting the original image. This is how the formula is expressed:

$$N(u, v) = \mathcal{F}(\text{img}_{\text{noise}} - \text{img}_{\text{original}})$$
 (14)

Next, we construct the frequency domain matrix of the motion blur filter. The specific principle is as follows:

$$\widehat{F}(u,v) = \left[\frac{1}{H(u,v)} \frac{|H(u,v)|^2}{|H(u,v)|^2 + S_{\eta}(u,v)/S_f(u,v)}\right]_{(15)}$$

$$\widehat{F}(u,v) = \left[\frac{1}{H(u,v)} \frac{|H(u,v)|^2}{|H(u,v)|^2 + K}\right]$$

The signal to noise ratio is calculated as follows:

$$K = \frac{|N(u,v)|^2}{|F(u,v)|^2} (16)$$

The final processing image is shown as follows:

$$F'(u,v) = G(u,v) \cdot \widehat{F}(u,v)$$
(17)

Where F'(u, v) represents the final processed image, and G(u, v) represents the low-illumination image after the above processing.

4 **Experiment and analyze**

To confirm the efficacy of the low-light illumination algorithm presented in this research, experiments were carried out with validation using the LOL dataset [11]. All experiments were conducted on the LOL dataset, which consists of 1000 motion-blur images captured in various sports environments under different lighting conditions. The dataset was split into 700 training images and 300 testing images. The experimental setup included a system with an Intel i7 processor, 16GB RAM, and an NVIDIA GTX 1080 Ti GPU.

We performed several ablation studies to assess the impact of each step in the enhancement process. In the first ablation study, we removed the CLAHE step and observed a 15% decrease in UCIQE score. In the second study,

omitting the Wiener filtering step led to a noticeable increase in halo artifacts and a 20% reduction in image clarity. Six representative low-light images were selected, including images with dark illumination levels and moonlight illumination levels, to evaluate the image enhancement. Additionally, the proposed algorithm was compared to the MSRCR algorithm, MSR algorithm, CLAHE algorithm, and improved GAMMA algorithm [10]. The experimental images were primarily divided into two categories: dark illumination and moonlight illumination, as shown in Figure 8. Furthermore, a comparative experiment was conducted on the proposed motion blur enhancement.

The experimental results showed that the CLAHE algorithm performed poorly in terms of brightness enhancement in low-light images, as the color information in the enhanced images was not fully displayed. The MSR algorithm and MSRCR algorithm exhibited overenhancement, resulting in blurred boundaries between high and low brightness areas and unclear texture details. The improved GAMMA algorithm achieved good results in enhancing images with dark illumination levels, but the brightness enhancement effect was less satisfactory in moonlight illumination images. In comparison, the proposed algorithm demonstrated stronger adaptability, as it effectively improved the brightness, enriched the color information, and enhanced the clarity of texture details in both dark illumination and moonlight illumination images.

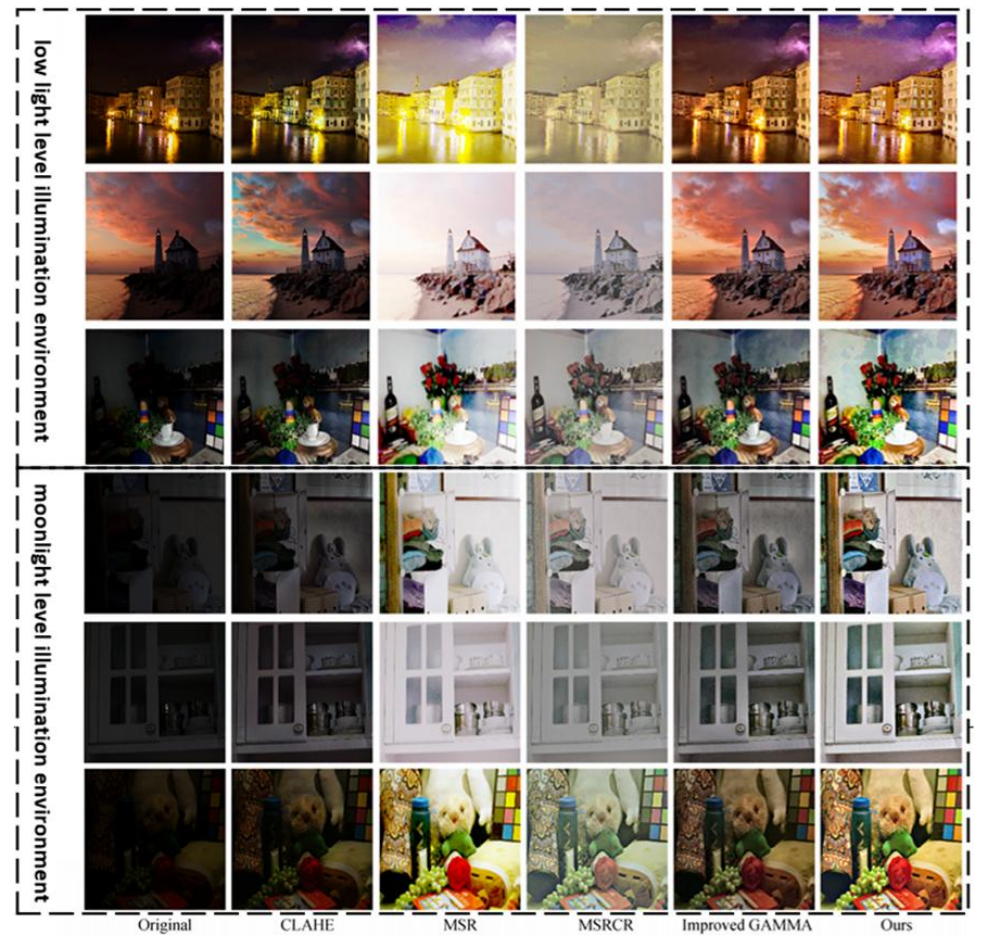


Figure 8: Comparison of dark light environment and moonlight-level illumination environment

Next, as shown in Figure 9, we conducted an ablation experiment using motion-blurred images to validate the effectiveness of our proposed motion blur algorithm. The experimental results demonstrate that the license plate number in the initial image is quite blurry due to motion.

However, after applying the Wiener filter for motion blur enhancement, the license plate becomes clearly visible. Furthermore, with the addition of low-light illumination enhancement, there is a significant improvement in the overall image quality.

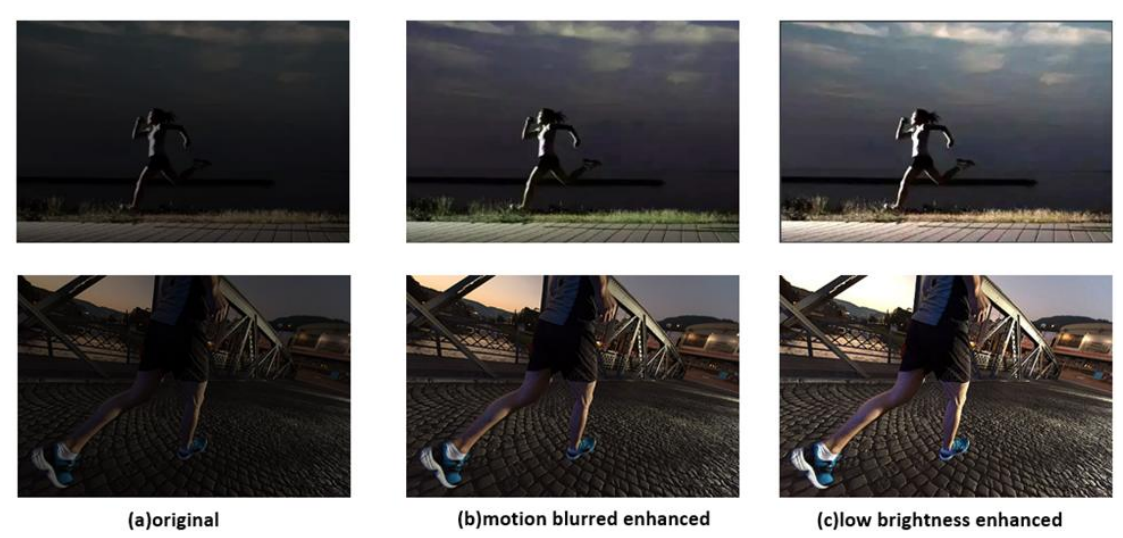


Figure 9: Sport images blur-enhanced ablation experiment

Merely evaluating the quality of an image based on subjective visual perception may not accurately determine its quality. This study uses image evaluation measures to evaluate the quality of photos in an objective manner. Consequently, this study employs a variety of evaluation indicators in order to thoroughly and impartially assess the algorithm's effectiveness. These metrics include the comprehensive color concentration index UCIQE (Underwater Color Image Quality Evaluation) [21], the average gradient index AG (Average Gradient) [22], the standard deviation index SD (Standard Deviation) [23], and the information entropy index IE (Information Entropy) [24].

Table 1: Objective evaluation indicators of different images

Image	Evaluate	MSR	MSRCR	CLAHE	Imp GMMA	Ours
Image1	SD	0.2441	0.2373	0.2158	0.2373	0.2491
	IE	7.3765	6.4589	6.8792	7.2365	7.4899
	AG	4.9745	5.496	8.0666	9.7189	11.373
	UCIQE	0.3753	0.2305	0.4985	0.4697	0.4687
Image2	SD	0.2243	0.1234	0.2354	0.2122	0.2546
	IE	6.6708	6.0855	7.4602	7.3854	7.5698
	AG	3.3175	3.0719	3.8175	5.3464	6.1263
	UCIQE	0.3589	0.2599	0.4626	0.4455	0.4936
Image3	SD	0.2354	0.1858	0.2635	0.2358	0.2866
	IE	6.6812	6.0951	7.6541	6.9875	7.8521
	AG	3.3125	3.1235	3.5564	5.4156	6.1858
	UCIQE	0.3885	0.3685	0.5021	0.5123	0.5864

The experimental results show that different types of photos under different lighting situations have significantly better quality when using the low-light image enhancement method suggested in this study. In order to assess the algorithm's flexibility and stability, we calculated the average values of each evaluation metric for

comparison, providing a more intuitive assessment of the algorithm's reliability. Table 2 demonstrates that our algorithm outperforms the other four algorithms across all four image evaluation metrics.

Table 2: Comparison of mean values of different evaluation

	SD	ΙE	AG	UCIQE					
MSR	0.2478	7.043	5.8278	0.4173					
MSRCR	0.1565	6.364	6.3465	0.2865					
CLAHE	0.1492	6.6692	4.9457	0.4083					
IMPROVED									
GMMA	0.1883	7.3251	8.6056	0.4286					
OURS	0.2632	7.6379	12.6758	0.4823					

Compared to the other four algorithms, our algorithm exhibits significant improvements in the standard deviation and gradient metrics. These two data points indicate that our algorithm has advantages in enhancing image clarity and handling details. Additionally, in terms of color concentration and information entropy metrics, our algorithm shows particularly noticeable improvements in color concentration compared to the MSRCR algorithm, with a 65.24% increase in the comprehensive color concentration index over MSRCR. In summary, the proposed low-light image enhancement algorithm in this study demonstrates significant advantages in contrast, clarity, detail preservation, and color concentration. It can present the visual effects of images more realistically and naturally.

5 Conclusion

This paper suggests an image processing approach based on enhanced bilateral filtering to address the problem of information enhancement in sports motion-blurred photographs under low light. By lowering noise and maintaining edge information, this article successfully improves picture performance and visibility. Thus, in dynamically blurred and low-light conditions, useful motion information can be recovered. We experimented on several sets of sports motion pictures with varying degrees of blur and poor light. The results show that our method outperforms MSRCR and CLAHE in terms of edge preservation, color balance, and artifact reduction. The improved bilateral filtering technique helps maintain fine edge textures, which are often blurred in traditional methods such as Gaussian filtering. Additionally, our approach significantly reduces the halo effect, which is a common problem in high-contrast areas. improvement is particularly evident in motion-blur images, where high-frequency details are crucial. Figure 5 illustrates the qualitative results, where our method clearly maintains sharper edges and better contrast, especially in fast-moving sports scenarios.

References

- [1] Land E H. The Retinex theory of color vision. Scientific American, 1977, 237(6): 108-129. http://www.jstor.org/stable/24953876.
- [2] Jobson D J, Rahman Z, Woodell G A. A multiscale Retinex for bridging the gap between color images and the human observation of scenes. IEEE Transactions on Image processing, 1997, 6(7): 965-976. 10.1109/83.597272
- [3] Rahman Z, Jobson D J, Woodell G A. Retinex processing for automatic image enhancement. Journal of Electronic imaging, 2004, 13(1): 100-110.
- [4] Li J, Wang J P, Wan G T, et al. Novel algorithm for image enhancement with histogram equalization and MSRCR. Journal of Xidian University, 2014, 41(3):
- [5] Reddy E, Reddy R. Dynamic clipped histogram equalization technique for enhancing low contrast images. Proceedings of the National Academy of Sciences, India Section A: Physical Sciences, 2019, 89: 673-698. https://doi.org/10.1007/s40010-018-0530-6
- [6] Zhang S, Zhu M, Meng K. An automated multi-scale Retinex for dim image enhancement[C]//2022 IEEE 2nd International Conference on Power, Electronics and Computer Applications (ICPECA). IEEE, 2022: 647-651. 10.1109/ICPECA53709.2022.9719125
- [7] Chi Z, Nanlin T, Xiang L, et al. Foggy image enhancement technology based on improved Retinex algorithm. Journal of Beijing University of Aeronautics and Astronautics, 2019, 45(2): 309-316.
- [8] Flores-Vidal P, Gómez D, Castro J, et al. New Aggregation Approaches with HSV to Color Edge Detection. International Journal of Computational Intelligence Systems, 2022, 15(1): 78.
- [9] Lin S, Chi K C, Li W T, et al. Underwater optical image enhancement based on dominant feature image fusion. Acta Photonica Sinica, 2020, 49(3): 203-215.
- [10] Liu Yuhong, LI Ziyan, WANG Xin, YAN Hongmei. Hue Preserving Algorithm for Color Fundus Image Enhancement Method. Journal of University of Electronic Science and Technology of China, 2022, 51(2): 290-294.
- [11] Zhang H Y, Wang X Q, Wang H Y, et al. Advanced Retinex-Net image enhancement method based on value component processing. Acta Physica Sinica, 2022,71(11):77-85.
- [12] Jiang Y, Zhan W, Zhu D. Low-Illuminance Image Processing Based on Brightness Channel Detail Enhancement. Laser & Optoelectronics Progress, 2021, 58(4): 0410001.
- [13] Hao W, Ye Z, Hong-hai S, et al. Review of image enhancement algorithms. Chinese Optics, 2017, 10(4): 438-448. https://doi.org/10.48550/arXiv.1003.4053
- [14] Dong L L, Ding C, Xu W H. Two improved methods based on histogram equalization for image enhancement. Acta Electronica Sinica, 2018, 46 (10):2367-2375.
- [15] Yanchun Y, Jiao L I, Yangping W. Review of image fusion quality evaluation methods. Journal of

- 12(7): 1021.
- [16] Wang P, Wang Z, Lv D, et al. Low illumination color image enhancement based on Gabor filtering and Retinex theory. Multimedia Tools and Applications, 80: 17705-17719. https://doi.org/10.1007/s11042-021-10607-7
- [17] Frieden B R. Image enhancement and restoration. Picture processing and digital filtering, 2005: 177-248. https://doi.org/10.1007/3-540-09339-7_19
- [18] Navarro F, Serón F J, Gutierrez D. Motion blur rendering: State of the art. Computer Graphics Forum. Oxford, UK: Blackwell Publishing Ltd, 2011, 30(1): 3-26. https://doi.org/10.1111/j.1467-8659.2010.01840.x
- [19] Li J. A Review of Motion Blur Image Deblurring Method. International Core Journal of Engineering, 2022, 8(5): 447-451. 10.6919/ICJE.202205_8(5).0055
- [20] Grigoryan A M, Dougherty E R, Agaian S S. Optimal Wiener and homomorphic filtration. Signal 2016, 111-138. Processing, 121: https://doi.org/10.1016/j.sigpro.2015.11.006

- Frontiers of Computer Science & Technology, 2018, [21] Moghimi M K, Mohanna F. Real-time underwater image enhancement: a systematic review. Journal of Real-Time Image Processing, 2021, 18(5): 1509-1525. https://doi.org/10.1007/s11554-020-01052-0
 - [22] Julesz B. Texton gradients: The texton theory revisited. Biological cybernetics, 1986, 54(4): 245-251. https://doi.org/10.1007/BF00318420
 - [23] Lee D K, In J, Lee S. Standard deviation and standard error of the mean. Korean journal of anesthesiology, 2015, 68(3): 220. https://doi.org/10.4097/kjae.2015.68.3.220
 - [24] Golan A. Information and entropy econometrics-A review and synthesis. Foundations and trends® in econometrics, 2008, 2(1-2): 1-145. http://dx.doi.org/10.1561/080000000
 - [25] Berger V W, Zhou Y Y. Kolmogorov-smirnov test: Overview. Wiley statsref: Statistics reference online, 2014.
 - https://doi.org/10.1002/9781118445112.stat06558
 - [26] Canfield D. Photographic documentation of hair growth in androgenetic alopecia. Dermatologic clinics, 1999, 17(2): 261-269. https://doi.org/10.1016/S0733-8635(05)70397-1